© 2017 IJSRSET | Volume 3 | Issue 6 | Print ISSN: 2395-1990 | Online ISSN : 2394-4099
Themed Section: Engineering and Technology

Effect of modification structure on some properties and corrosion behavior of Bi- Sn- Pb- Cd alloys for shielding blocks

A. B. El-Bediwi[1], M.D. Khalaf[2*], Kh.M. Omar[3], T.M. Meaz[4]
[1]Physics Department, Faculty of Science, Mansoura University, Egypt
[2*,3,4]Physics Department, Faculty of Science, Tanta University, Egypt

ABSTRACT

The aim of our research was to decrease the toxic metals (cadmium and lead) from Bi- Sn- Pb- Cd alloy with improve properties\ or produce new friendly environmental alloy with superior properties and low coast. To verify these aims, microstructure, thermal behavior and electrochemical corrosion parameters of normal casting Bi- Sn- Pb- Cd alloys have been investigated. Cadmium decreased by 70% and lead by 60% from original alloy. The results show corrosion resistance of Bi- Pb- Sn- Cd alloys increased with decreased Pb and Cd contents. Thermal parameters and lattice micro-strain of $Bi_{50}Pb_{25}Sn_{12.5}Cd_{12.5}$ alloy decreased by decreasing Pb and Cd. $Bi_{58}Pb_{10}Sn_{28}Cd_4$ alloy has best properties and friendly environmental.

Keywords: Corrosion Parameters, Microstructure, Thermal Behavior, Density

I. INTRODUCTION

Fusible alloys have great importance for medical and industrial applications. They contained bismuth, lead, tin, cadmium or indium as fusible elements in safety devices [1-3], alarms, radio-opaque contrast medium in x-ray, low temperature solder and nuclear medicine as a shielding block [4]. Shepelevich et al [5] reported the structure, mechanical properties and thermal stability of Sn-58 wt. % Bi alloys produced by melt cooling at rate above 10k/s. Also the solubility of Bi in Sn for binary Bi-Sn system was studied using SEM/EDS, DTA/DSC and RT-XRD [6] and the results show that, Sn dissolves approximately 10 wt. % of Bi at the eutectic temperature. El-Bediwi et al [7] reported that, thermal behavior and physical properties of $Bi_{75}Pb_{25}$, $Bi_{87.5}Sn_{12.5}$, $Bi_{87.5}Cd_{12.5}$ and $Bi_{62.5}Pb_{25}Sn_{12.5}$, $Bi_{75}Sn_{12.5}Cd_{12.5}$, $Bi_{62.5}Pb_{25}Cd_{12.5}$ alloys changed correlated to the formation of hexagonal Pb_7Bi_3 intermetallic compound and solid solution. Also microstructure, thermal, electrical and mechanical properties of $Bi_{50}Pb_{15}Sn_{22}In_{10}X_3$, $Bi_{50}Pb_{15}Sn_{28}In_4X_3$ (X=Cd or Zn), $Bi_{45.5}Sn_{42}Pb_3Zn_3In_4Ag_{2.5}$, $Bi_{25}Sn_{62.5}Pb_3Zn_3In_4Ag_{2.5}$ and $Bi_{50-x}Pb_{15}Sn_{22}Cd_3In_{10}(TiO_2)_x$(x= 0.5, 1, 1.5) alloys depend on alloys compositions [8, 9]. El-Bediwi et al [10] studied microstructure and solder properties of tin- bismuth- X (X= Cu and Ag), tin- bismuth- X (X = Zn-In, Zn-Cu, Cu-In, Sb-In and Ag- In) and tin- bismuth- X (X=Ag-In-TiO_2) alloys. They studied the microstructure, some physical properties of $Bi_{50-x}Pb_{15}Sn_{22}Cd_3In_{10}(TiO_2)_x$[x=0.5-1.5], $Bi_{45.5}Sn_{42}Pb_3Zn_3In_4Ag_{2.5}$ and $Bi_{25}Sn_{62.5}Pb_3Zn_3In_4Ag_{2.5}$ alloys [11]. The results show all measured properties dependent on alloy composition. Also they reported that there is a significant increase in bismuth-tin-zinc alloy strengthens after adding silver but a significant decrease in its melting point after adding indium [12]. El-Bediwi et al [13] studied the microstructure, electrochemical corrosion behavior, thermal parameters and wettability of $Sn_{50}Bi_{30}Sb_{10}Al_5Zn_3Cu_2$, $Sn_{61}Bi_{25}Sb_5Zn_4Al_3Ag_2$ and $Sn_{60}Bi_{20}Sb_7Al_5Zn_3Cd_3Cu_2$ alloys. Therefore, the objective of this research was to understand the correlation between thermal behavior and electrochemical corrosion parameters with alloy composition to produce friendly environmental shielding blocks alloy.

II. METHODS AND MATERIAL

Bismuth, lead, tin and cadmium metals with purity more than 99.9 % were used to prepare $Bi_{50}Pb_{25}Sn_{12.5}Cd_{12.5}$, $Bi_{55}Pb_{20}Sn_{15}Cd_{10}$, $Bi_{55}Pb_{15}Sn_{20}Cd_{10}$, $Bi_{57.5}Pb_{10}Sn_{25}Cd_{7.5}$ and

$Bi_{58}Pb_{10}Sn_{28}Cd_4$ alloys. These alloys (mixed metals with different ratio) were melted and then normal casted on copper substrate in air. For all tests as structure, thermal parameters and corrosion behavior, the samples were prepared in convenient shape. Microstructure of used alloys was performed using Shimadzu X–ray Diffractometer (Dx–30, Japan) Cu–Kα radiation with λ=1.54056 Å at 45 kV and 35 mA and Ni–filter, in the angular range 2θ ranging from 0 to 100° in continuous mode with a scan speed 5 deg./min and scanning electron microscope (JEOL JSM-6510LV, Japan). The polarization studies were performed using Gamry Potentiostat/Galvanostat with a Gamry framework system based on ESA 300. Gamry applications include software DC105 for corrosion measurements, and Echem Analyst version 5.5 software packages for data fitting. The differential scanning calorimeter (DSC) thermographs were obtained by Universal V4. 5A TA Instrument with heating rate 10 k/min in the temperature range 0-400 °C

III. RESULTS AND DISCUSSION

A. X-ray Analysis

X-ray diffraction patterns of $Bi_{50}Pb_{25}Sn_{12.5}Cd_{12.5}$, $Bi_{55}Pb_{20}Sn_{15}Cd_{10}$, Bi_{55} $Pb_{15}Sn_{20}Cd_{10}$, $Bi_{57.5}Pb_{10}Sn_{25}Cd_{7.5}$ and $Bi_{58}Pb_{10}Sn_{28}Cd_4$ alloys have lines corresponding to different phases as shown in Figure 1. Data from x-ray devise (2θ, d, FWHM and intensity) and cards (phase and hkl) are listed in Table 1. From x-ray analysis, the used alloys contained rhombohedral Bi phase, tetragonal Sn phase, face centered cubic Pb phase, hexagonal Cd phase, Pb_7Bi_3 and SnBi intermetallic compounds with different crystallinty (peak intensity), crystal size (peak broadness) and orientation (peak position) which dependent on alloy composition. Lattice microstain of $Bi_{50}Pb_{25}Sn_{12.5}Cd_{12.5}$, $Bi_{55}Pb_{20}Sn_{15}Cd_{10}$, Bi_{55} $Pb_{15}Sn_{20}Cd_{10}$, $Bi_{57.5}Pb_{10}Sn_{25}Cd_{7.5}$ and $Bi_{58}Pb_{10}Sn_{28}Cd_4$ alloys were calculated from the relation between full half width maximum (FHWM) and 4tanθ [14] then presented in Figure 2. Lattice microstrain of $Bi_{50}Pb_{25}Sn_{12.5}Cd_{12.5}$ alloy decreased by decreasing Pb and Cd as listed in Table 2.

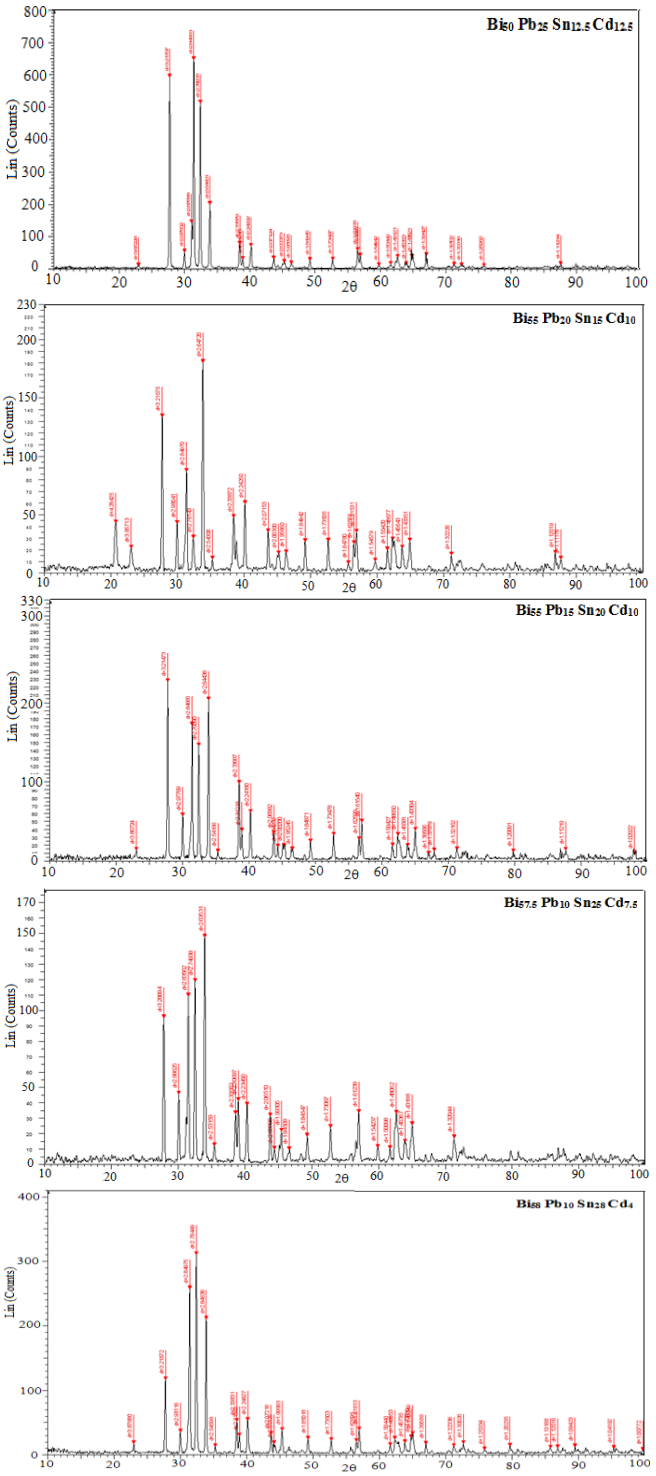

Figure 1: x-ray diffraction patterns of Bi- Pb- Sn- Cd alloys

Table 1: x-ray diffraction analysis of Bi- Pb- Sn- Cd alloys

Bi_{50} Pb_{25} $Sn_{12.5}$ $Cd_{12.5}$				
2θ	d Å	Int. %	phase	hkl
22.948	3.87228	1.2	Bi	003
27.707	3.21707	91.6	Bi	012
29.981	2.97802	7.8	Sn	200
31.061	2.87688	21.9	Pb_7Bi_3	002
31.4	2.84663	100	Sn	200
32.412	2.76005	79.1	Sn	101

33.876	2.64401	30.6	Pb_7Bi_3	101
38.46	2.33879	11.6	Cd	101
38.92	2.31218	4.4	Cd	101
40.173	2.24292	10.7	Bi	110
43.666	2.07124	4.5	Sn	220
45.289	2.00073	2.9	Bi	006
46.36	1.95695	2.2	Bi	006
49.228	1.84945	3.8	Bi	202
52.717	1.73497	4.1	Pb	220
56.541	1.62635	8.7	Bi	024
56.944	1.61581	5.9	Bi	024
59.794	1.54542	1.3	Bi	107
61.597	1.50442	2.1	Bi	205
62.671	1.48121	5.3	Pb	311
63.99	1.45383	1.9	Sn	400
64.87	1.43621	5.3	Sn	321
67.074	1.39427	6.2	Bi	018
71.339	1.32102	1.6	Bi	009
72.47	1.30316	1.2	Cd	200
75.897	1.25262	1.1	Bi	303
87.657	1.11234	1.8	Bi	217

35.284	2.54166	4.7	Cd	100
38.493	2.33687	43	Cd	101
38.92	2.31218	16.4	Cd	101
40.194	2.2418	26.8	Bi	110
43.695	2.06992	14.9	Sn	220
44.317	2.04232	7.5	Bi	015
45.258	2.002	7.7	Sn	211
46.473	1.95245	5.8	Bi	006
49.249	1.84871	10.3	Bi	202
52.723	1.73478	14.1	SnBi	301
56.555	1.62599	11.7	Bi	024
56.96	1.6154	21.5	Bi	024
61.604	1.50427	8.1	Bi	205
62.423	1.4865	13.9	Pb	311
63.892	1.45581	7.9	Sn	400
65.031	1.43304	16.9	Sn	321
67.031	1.39506	3.3	Bi	018
67.874	1.37978	5.2	Bi	018
71.302	1.32162	6	Bi	009
79.797	1.20091	4.7	Pb	400
87.672	1.11219	5.7	Bi	217
98.056	1.02022	3.2	Bi	134

$Bi_{55}Pb_{20}Sn_{15}Cd_{10}$				
2θ	d Å	Int. %	phase	hkl
20.716	4.28425	23.6	Bi	
23.04	3.85713	11.5	Bi	003
27.719	3.21575	74.1	Bi	012
29.957	2.98041	23.3	Sn	200
31.365	2.8497	48	Pb	111
32.395	2.76143	16.3	Sn	101
33.834	2.6472	100	Pb_7Bi_3	101
35.264	2.54308	6.3	Cd	100
38.461	2.33872	26.1	Cd	101
40.181	2.2425	32.7	Bi	110
43.66	2.07153	19.3	Sn	220
45.234	2.003	8.9	Sn	211
46.369	1.9566	9.3	Bi	006
49.229	1.84942	14.6	Bi	202
52.714	1.73505	14.8	SnBi	301
55.741	1.6478	4.1	Bi	024
56.57	1.62559	13.6	Bi	024
56.963	1.61531	19.1	Bi	024
59.778	1.54579	5.4	Bi	107
61.608	1.5042	10.7	Bi	205
62.41	1.48677	15.5	Pb	311
63.862	1.45643	11.6	Sn	400
65.007	1.43351	14.8	Bi	122
71.262	1.32226	8.2	Bi	009
86.889	1.12019	9.1	SnBi	520
87.714	1.11176	6.2	Bi	217

$Bi_{57.5}Pb_{10}Sn_{25}Cd_{7.5}$				
2θ	d Å	Int. %	phase	hkl
27.85	3.20094	64.3	Bi	012
30.103	2.96625	30.7	Pb_7Bi_3	100
31.525	2.83562	73.9	Pb	111
32.541	2.74938	80.5	Sn	101
33.991	2.63531	100	Pb_7Bi_3	101
35.429	2.53159	7.9	Cd	100
38.602	2.33052	22	Cd	101
39.012	2.30697	27.8	Bi	110
40.331	2.2345	25.8	Bi	110
43.802	2.0651	21	Sn	220
44.437	2.03708	6.3	Bi	015
45.473	1.99305	14.3	Bi	113
46.66	1.94509	6	Bi	021
49.341	1.84547	12.1	Bi	202
52.851	1.73087	16	SnBi	301
57.076	1.61239	22.5	Bi	024
59.924	1.54237	7.2	Bi	205
61.754	1.50098	6.6	Bi	205
62.699	1.48062	22.2	Pb	311
63.997	1.45367	9.5	Sn	400
65.09	1.43188	17.1	Bi	122
71.375	1.32044	11.4	Bi	009

$Bi_{55}Pb_{15}Sn_{20}Cd_{10}$				
2θ	d Å	Int. %	phase	hkl
22.979	3.86724	5.7	Bi	003
27.728	3.21473	100	Bi	012
29.985	2.97769	24.7	Sn	200
31.4	2.84666	75.6	Pb	111
32.401	2.7609	64.1	Sn	101
33.871	2.64438	89.7	Pb_7Bi_3	101

$Bi_{58}Pb_{10}Sn_{28}Cd_4$				
2θ	d Å	Int. %	phase	hkl
22.921	3.8768	5.3	Bi	003
27.693	3.21872	37.2	Bi	012
29.949	2.98116	11	Pb_7Bi_3	100
31.365	2.84975	82.8	Sn	200
32.358	2.76449	100	Sn	101

33.845	2.64636	67.6	Pb_7Bi_3	101
35.222	2.54599	3.7	Cd	100
38.468	2.33831	16.5	Cd	101
38.86	2.31562	9	Cd	101
40.11	2.24627	16.9	Bi	110
43.645	2.07218	9.9	Sn	220
44.068	2.05326	5.1	Sn	220
45.308	1.99993	11.9	Bi	113
49.207	1.85018	7.5	Bi	202
52.715	1.73503	6.8	SnBi	301
56.519	1.62695	6.3	Bi	024
56.931	1.61613	12.1	Bi	024
61.598	1.5044	4.2	Bi	205
62.328	1.48853	7.4	Pb	311
63.817	1.45735	5.8	Sn	400
64.764	1.4383	8.1	Sn	321
65.008	1.43349	9.8	Sn	321
66.986	1.39589	4.9	Bi	018
71.194	1.32336	3.8	Bi	214
72.658	1.30026	5.3	Bi	300
75.845	1.25334	2	Cd	201
79.683	1.20235	4	Pb	400
85.773	1.13188	3	Bi	220
86.892	1.12016	3.2	Bi	217
89.492	1.09423	3.6	Bi	306
95.345	1.04192	2.8	Bi	134
99.706	1.00772	1.9	Bi	315

Table 2: lattice microstrain of Bi- Pb- Sn- Cd alloys

Alloys	ε
$Bi_{50}Pb_{25}Sn_{12.5}Cd_{12.5}$	0.293
$Bi_{55}Pb_{20}Sn_{15}Cd_{10}$	0.016
$Bi_{55}Pb_{15}Sn_{20}Cd_{10}$	0.021
$Bi_{57.5}Pb_{10}Sn_{25}Cd_{7.5}$	0.077
$Bi_{58}Pb_{10}Sn_{28}Cd_4$	0.072

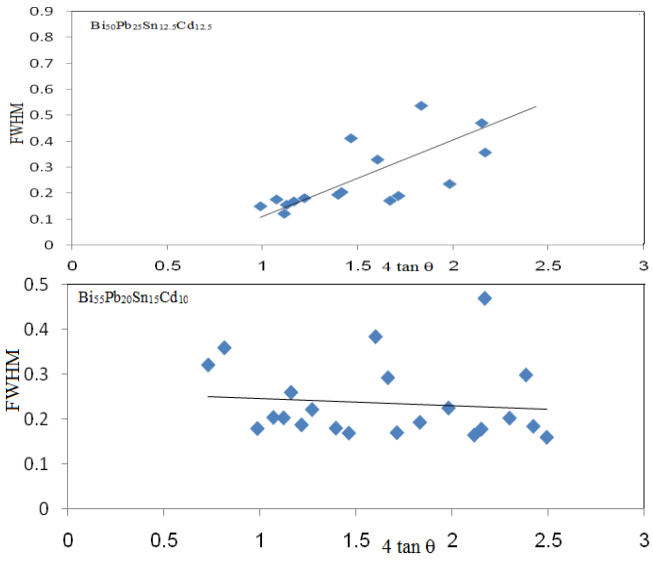

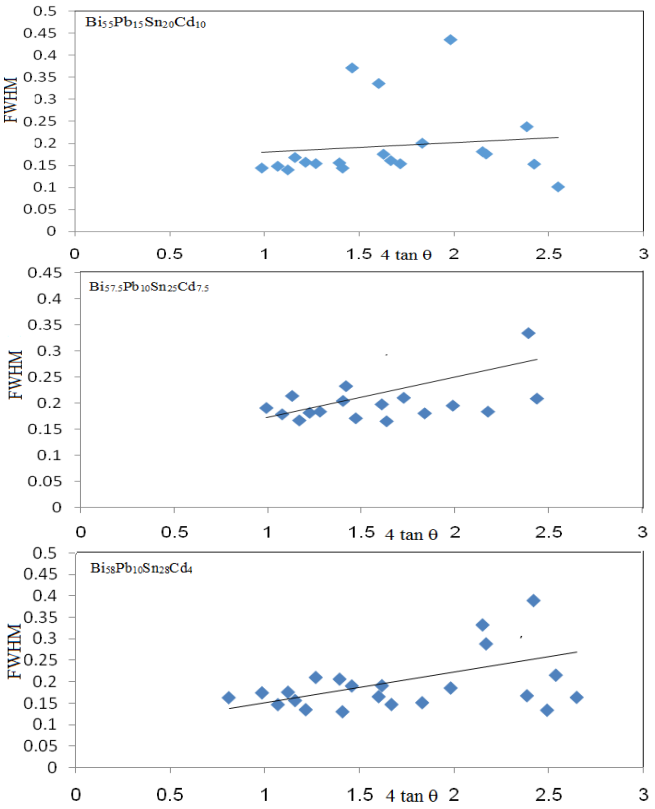

Figure 2: FWHM versus 4 tanθ for Bi- Pb- Sn- Cd alloys

B. Scanning electron microscope analysis

Scanning electron microscope graphs of $Bi_{50}Pb_{25}Sn_{12.5}Cd_{12.5}$, $Bi_{55}Pb_{20}Sn_{15}Cd_{10}$, Bi_{55} $Pb_{15}Sn_{20}Cd_{10}$, $Bi_{57.5}Pb_{10}Sn_{25}Cd_{7.5}$ and $Bi_{58}Pb_{10}Sn_{28}Cd_4$ alloys are shown in Figure 3. $Bi_{50}Pb_{25}Sn_{12.5}Cd_{12.5}$ alloy has heterogeneous structure, bismuth as a lamellar structure with different shape and orientation (gray color), tin as a separate or interference spherical shape (black color) and small spherical grains (lead or cadmium or intermetallic compound) around matrix grains or dispersed in it (white color). $Bi_{55}Pb_{20}Sn_{15}Cd_{10}$ alloy has a lamellar structure (gray color), rods and spherical shapes (black color) and a little small rods (white color) disturbed in matrix. Bi_{55} $Pb_{15}Sn_{20}Cd_{10}$ alloy has mixed from spherical and cylindrical shape (gray color), rods shape with different length and orientation (black color) and a little rods shape (white color) disturbed in matrix. $Bi_{57.5}Pb_{10}Sn_{25}Cd_{7.5}$ alloy has heterogeneous structure from gray color and black color which have a little cylindrical rods (white color). $Bi_{58}Pb_{10}Sn_{28}Cd_4$ alloy has interference lamellar structure with different shape, size and orientation (gray color) contained spherical small grains (black color) and white color a long grain boundary of gray grains. From the results, it is obvious

that, modified structure (by changed the ratio of elements) of Bi- Pb- Sn- Cd caused a change in microstructure like shape, size and orientation of formed phases.

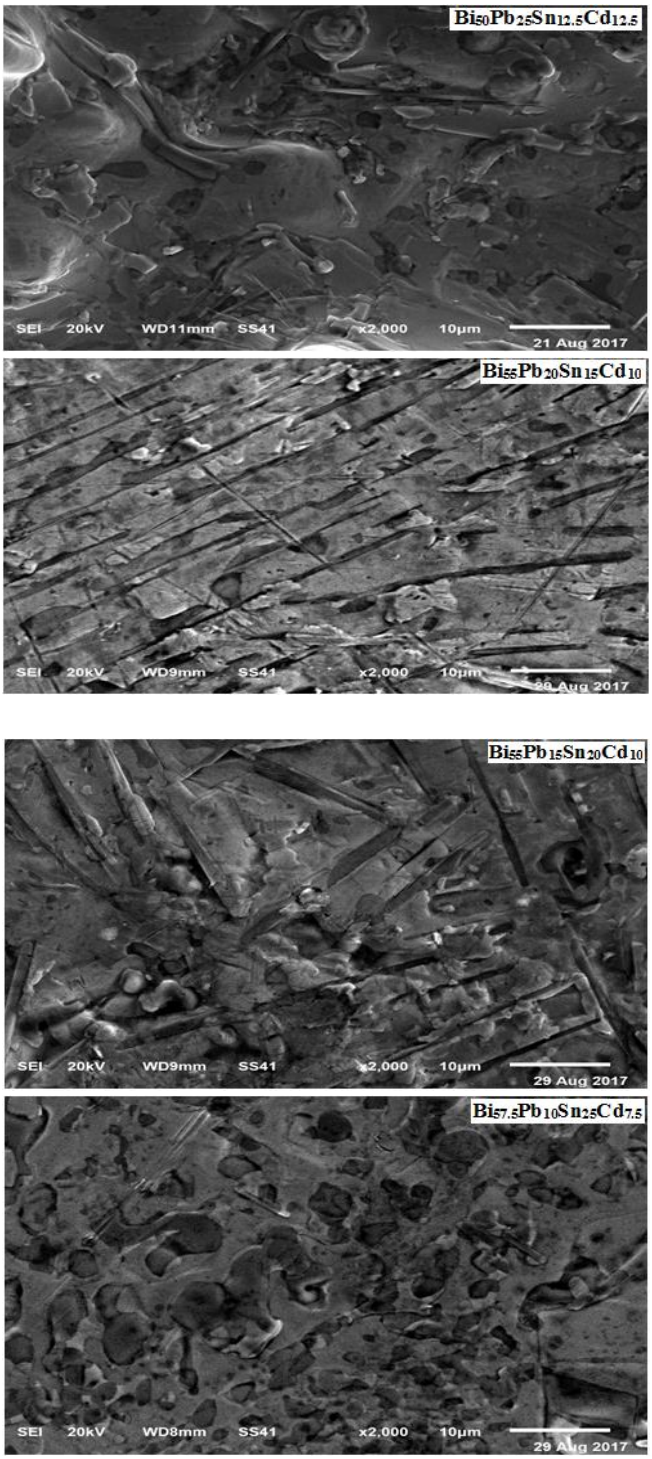

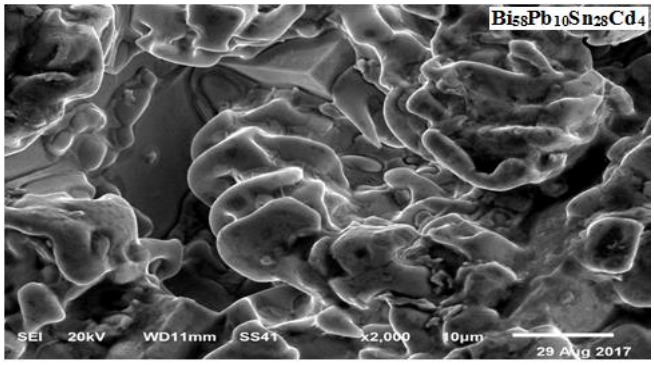

Figure 3: SEM of Bi- Pb- Sn- Cd alloys

C. Density measurements

A material's density is defined as its mass per unit volume. It is, essentially, a measurement of how tightly matter is packed together. The change in density can also be useful in analyzing some situations, such as whenever a chemical conversion is taking place and energy is being released. Experimental and theoretical calculation of density for $Bi_{50}Pb_{25}Sn_{12.5}Cd_{12.5}$, $Bi_{55}Pb_{20}Sn_{15}Cd_{10}$, Bi_{55} $Pb_{15}Sn_{20}Cd_{10}$, $Bi_{57.5}Pb_{10}Sn_{25}Cd_{7.5}$ and $Bi_{58}Pb_{10}Sn_{28}Cd_4$ alloys are listed in Table 3. The density value of Bi- Pb- Sn- Cd alloy decreased with lead and cadmium content decreased except at $Bi_{58}Pb_{10}Sn_{28}Cd_4$ alloy.

Table 3: experimental and theoretical calculation of density for used alloys

Alloys	ρ gm/cm^3 (Theatrical)	ρ gm/cm^3 (Experimental)
$Bi_{50}Pb_{25}Sn_{12.5}Cd_{12.5}$	9.76	10.22
$Bi_{55}Pb_{20}Sn_{15}Cd_{10}$	9.65	10.03
$Bi_{55}Pb_{15}Sn_{20}Cd_{10}$	9.45	9.63
$Bi_{57.5}Pb_{10}Sn_{25}Cd_{7.5}$	9.27	9.15
$Bi_{58}Pb_{10}Sn_{28}Cd_4$	9.24	9.39

D. Thermal properties

It is very important to study the response of a material to heat. The melting point is dissimilar for different materials and for each material it slightly varies when the superincumbent pressure varies. The alloys have a range of melting and not a fixed melting temperature but the eutectic alloys have fixed melting point. The melting temperature of a solid material depends on the interatomic and intermolecular bonds. Materials having stronger bonds exhibit higher melting points. The differential scanning calorimeter, DSC, curve (endothermic/exothermic) is used for detecting and

characterizing thermal processes qualitatively. Figure 4 shows differential scanning micrographs of $Bi_{50}Pb_{25}Sn_{12.5}Cd_{12.5}$, $Bi_{55}Pb_{20}Sn_{15}Cd_{10}$, Bi_{55} $Pb_{15}Sn_{20}Cd_{10}$, $Bi_{57.5}Pb_{10}Sn_{25}Cd_{7.5}$ and $Bi_{58}Pb_{10}Sn_{28}Cd_4$ alloys. DSC graphs show the thermal behavior, (Endothermic peaks shape, position and intensity), of $Bi_{50}Pb_{25}Sn_{12.5}Cd_{12.5}$ alloy changed. Entropy, enthalpy and specific heat capacity of Bi- Pb- Sn- Cd alloys decreased with the amount of Pb and Cd decreased as shown in Table 4. That is meant the atoms disorder and matrix defects in a system decreased and it's agreed with the lattice microstrain results.

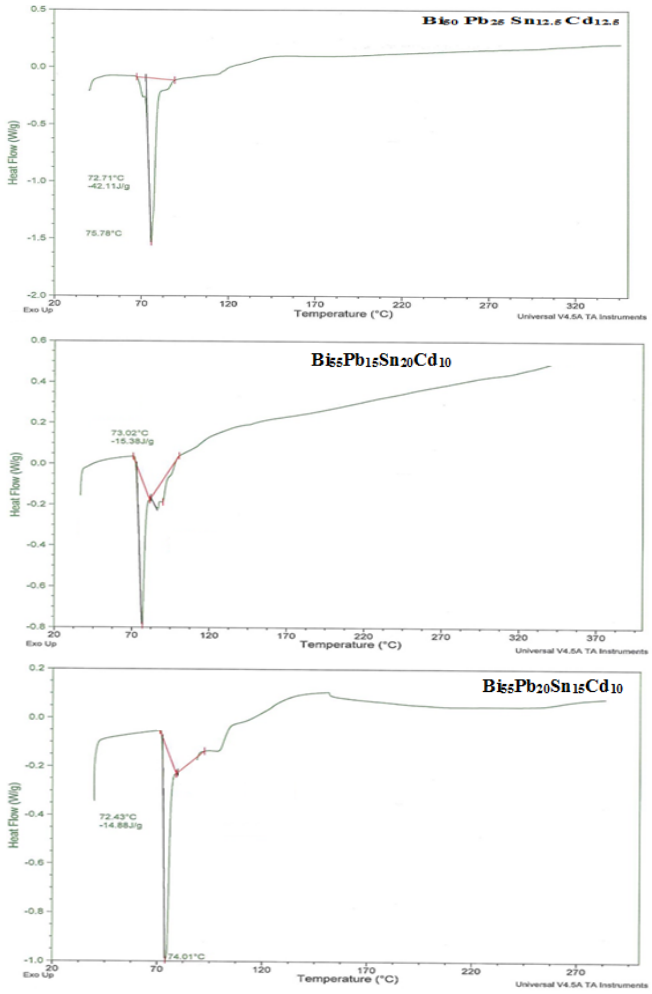

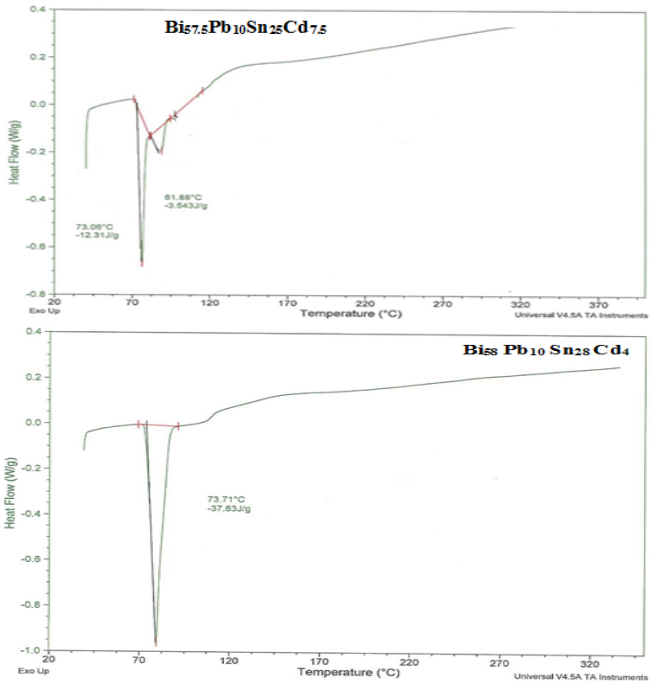

Figure 4: DSC graphs of Bi- Pb- Sn- Cd alloys

Table 4: thermal parameters of Bi- Pb- Sn- Cd alloys

Alloys	Melting temperature ^oC	C_p J/g. °C	H_c J/g	S J/°C
$Bi_{50}Pb_{25}Sn_{12.5}Cd_{12.5}$	75.75	2.22	42.1	0.55
$Bi_{55}Pb_{20}Sn_{15}Cd_{10}$	74.01	0.61	14.9	0.18
$Bi_{55}Pb_{15}Sn_{20}Cd_{10}$	73.02	0.295	15.4	0.11
$Bi_{57.5}Pb_{10}Sn_{25}Cd_{7.5}$	73.06	0.279	12.3	0.14
$Bi_{58}Pb_{10}Sn_{28}Cd_4$	73.71	1.182	37.8	0.34

E. Electrochemical corrosion behavior

Figure 5 shows electrochemical polarization curves of $Bi_{50}Pb_{25}Sn_{12.5}Cd_{12.5}$, $Bi_{55}Pb_{20}Sn_{15}Cd_{10}$, Bi_{55} $Pb_{15}Sn_{20}Cd_{10}$, $Bi_{57.5}Pb_{10}Sn_{25}Cd_{7.5}$ and $Bi_{58}Pb_{10}Sn_{28}Cd_4$ alloys. The corrosion potential of Bi- Pb- Sn- Cd alloys showed a negative potential besides the cathodic and the anodic polarization curves exhibited similar corrosion trends. The corrosion current (I_{Corr}), corrosion potential (E_{Corr}) and corrosion rate ($Corr_{rate}$) of Bi- Pb- Sn- Cd alloys in 0.25 M HCl are obtainable in Table 5. Corrosion rate and corrosion current values of Bi- Pb- Sn- Cd alloys varied (decreased) by increasing Bi and Sn content and decreasing Pb and Cd content. That is because changing alloy composition caused a heterogeneous microstructure with affected on microsegregation and reactivity of atoms with HCl solution.

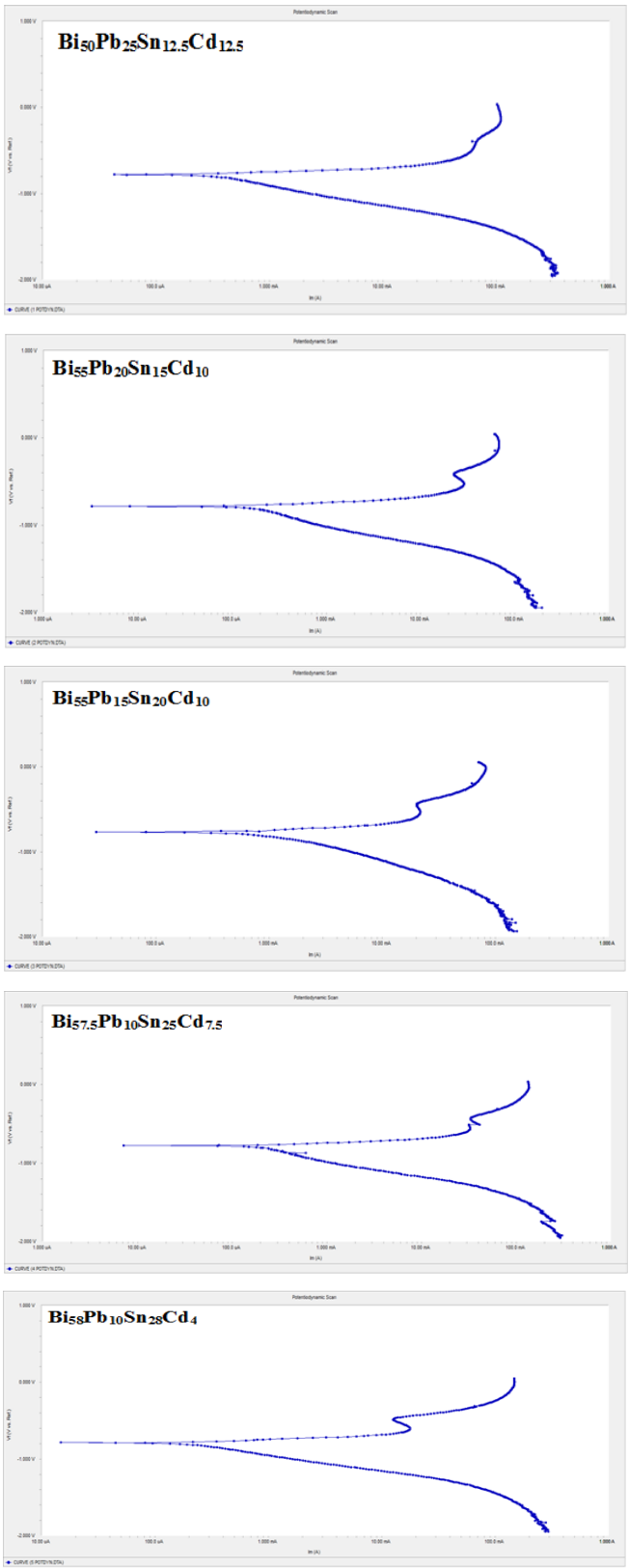

Figure 5: electrochemical polarization curves of Bi- Pb- Sn- Cd alloys

Table 5: corrosion parameters of Bi- Pb- Sn- Cd alloys

Alloys	I_{corr} µA	E_{corr} mv	$Corr_{rate}$ mpy
Bi_{50} Pb_{25} $Sn_{12.5}Cd_{12.5}$	325	-778	340.1
Bi_{55} Pb_{20} Sn_{15} Cd_{10}	141	-783	148
Bi_{55} Pb_{15} Sn_{20} Cd_{10}	259	-766	298.9
$Bi_{57.5}$ Pb_{10} Sn_{25} $Cd_{7.5}$	162	-780	169.2
Bi_{58} Pb_{10} Sn_{28} Cd_{4}	199	-788	208.5

IV. Conclusions

Matrix microstructure, formed phases, of Bi- Pb- Sn- Cd alloys dependent on their composition. A little decreased occurred in Bi- Pb- Sn- Cd alloys densities with decreased Pb and Cd contents. Corrosion rate of Bi- Pb- Sn- Cd alloys decreased by decreasing Pb and Cd contents. Entropy, enthalpy, specific heat capacity and lattice microstrain of Bi- Pb- Sn- Cd alloys decreased with the amount of Pb and Cd decreased. Our concluded that, it can produce new friendly environmental Bi- Pb- Sn- Cd shielding blocks alloy.

V. REFERENCES

[1]. M. T. McCormack, Y. Degani, H.S. Chen, W.R. Gesick, J. JOM, 48 (1996) 54

[2]. I. Manna and S.K. Pabi, Phys.Status Solidi A 123 (1991) 393

[3]. J. Perkins and G.R. Edwards, J. Mater. Sci. 10 (1975) 136

[4]. C.R. Blackwell and K.D.Andmunson, Med. Dosimetry 15 (1990)127

[5]. Shepelevich, O.V. Gusakova and L.P. Shcherba chenko, Inorganic Mater. 1:49: 7 (2013) 663

[6]. M.H. Braga, G. Bizdal, A. Krouba, G. Ferreira, D. Soares, L.F. Malheiros, (2007) 468

[7]. A.B. El-Bediwi, F. Dawood, M. Kamal, MSAIJ, 11: 5 (2014) 179

[8]. A.B. El-Bediwi, F. Dawood, M. Kamal, IJSEA. 4:2 (2015) 60

[9]. A.B. El-Bediwi, F. Dawood, M. Kamal, IJCR. 7: 5 (2015) 16433-16439

[10]. A.B. El-Bediwi, A. El-Shafei, M. Kamal, IJCR. 7: 6 (2015) 17305-17311

[11]. A.B. El-Bediwi, F. Dawood, M. Kamal, IJ CR. 7: 5 (2015) 16433-16439

[12]. A.B. El-Bediwi, F. Dawood, M. Kamal, J Advance Phys. 7:3 (2015)

[13]. A.B. El-Bediwi, S. Bader, F. Khalifa, Global Journal of Physics, 4: 3 (2016) 480

[14]. G.K. Williamson and W.H. Hall, Acta Metallurgy, 1 (1953) 22-31